

Effect of electro-thermo-mechanical coupling on the short-circuit in RF microswitch operation

*Original*

Effect of electro-thermo-mechanical coupling on the short-circuit in RF microswitch operation / Brusa, Eugenio; Munteanu, M. G. h.. - STAMPA. - 8066:(2011), pp. 80660W-1-80660W-15. (Intervento presentato al convegno SPIE Microtechnologies 2011 tenutosi a Prague (CZ) nel 18-20 April 2011) [10.1117/12.886595].

*Availability:*

This version is available at: 11583/2428579 since:

*Publisher:*

SPIE

*Published*

DOI:10.1117/12.886595

*Terms of use:*

This article is made available under terms and conditions as specified in the corresponding bibliographic description in the repository

*Publisher copyright*

(Article begins on next page)

# Effect of electro-thermo-mechanical coupling on the short-circuit in RF microswitch operation

E. Brusa<sup>\*a</sup>, M. Gh. Munteanu<sup>b</sup>

<sup>a</sup>Dept. Mechanics, Politecnico di Torino, C.so Duca degli Abruzzi, 24, 10129 Torino, Italy

<sup>b</sup>DIEGM, University of Udine, via delle Scienze, 208, 33100 Udine, Italy

## ABSTRACT

A phenomenological approach is herein followed to describe several superimposed effects occurring within the structure of microswitch for radio frequency application (RF-MEMS). This device is operated via a nonlinear electromechanical action imposed by applied voltage. Unfortunately, it is usually affected by residual stress, after microfabrication, therefore axial and flexural behaviors are coupled. This coupling increases actuation voltage to achieve the so-called “pull-in” condition. Moreover, temperature may strongly affect strain and stress distributions, respectively. Environmental temperature, internal dissipation of material, thermo-elastic and Joule effects play different roles on the microswitch flexural displacement. Sometimes buckling phenomenon evenly occurs. Finally, if stress concentration on microbeam cross section is sufficiently large, plastic behavior may arise. All those aspects make difficult an effective computation of pull-in voltage, understanding actual behavior of microsystem, particularly when several loading cycles are applied, and predicting its life. Analysis, experiments and numerical methods are herein applied to test case suggested by industry to investigate step by step the microswitch operation. Effects on pull-in and switch contact are investigated. Multiple electro-thermo-mechanical coupling is finally modeled to have a preliminary and comprehensive description of microswitch behavior and of its structural reliability.

**Keywords:** Structural reliability, thermomechanical coupling, electromechanical coupling, finite element method, buckling, microbridge, pull-in effect.

## 1. INTRODUCTION

Reliability prediction of Radio Frequency-Micro Electro Mechanical System, in following simply referred to as RF-MEMS, is rather difficult since several coupling effects are superimposed in operating conditions. Among several layouts already available<sup>[5]</sup>, microswitch is a relevant test case for design activity. Therefore this paper is expressively focused on this microdevice. Literature show that damage mechanisms are basically depending on plastic behavior of material, static rupture, fatigue even in presence of thermal effects, fracture, wear and electric failures<sup>[15,27-29,31-34,37,41]</sup>. Mechanical design of microswitch consequently requires an extensive experimental activity<sup>[22]</sup> mainly aimed at identifying some operation critical conditions and strength of materials at microscale<sup>[27,33,37]</sup>. Some tests are performed to characterize MEMS geometry, its functionality, like in case of “pull-in” and “pull-out” detection, and mechanical and physical properties of MEMS material, after microfabrication process, are identified. Particular care is applied to perform fatigue, fracture propagation and creep tests, to allow a consistent prediction of RF-MEMS life. Unfortunately, testing at microscale looks significantly more complicated than at macro and meso scales, because loading is often applied to the MEMS structure by resorting to electromechanical coupling, as is in case of electrostatic actuation of microbridges<sup>[9,19,24]</sup>. Recent contributions dealt with many aspects of design and experimental issues of microswitch operation, either used as a specimen at microscale to test and characterize materials<sup>[22,27,37]</sup> or as a RF-MEMS device fully integrated into an electronic circuit for communication systems<sup>[5]</sup>. A detailed analysis of electromechanical nonlinear coupling in statics and dynamics was already accomplished by several authors<sup>[7,9,11,12,20,21,24,25]</sup>, as well as a good experience in electromechanical actuation in presence of environmental fluidic action was even documented<sup>[35]</sup>. More recently industrial interest was focused on temperature role in microswitch reliability<sup>[3,13-15,17,36,39,41,43]</sup> and failure modes associated with temperature effects<sup>[26-31,36,39]</sup>. Quite seldom a complete electro-thermo-mechanical coupling was investigated<sup>[6,15,32,39]</sup>. Moreover, sometimes modeling, experimental and practice activities already available in some references and concerning multiple coupling effects show different results and claims about the MEMS performance.

\*Laboratory of Design and Characterization of Microsystems – eugenio.brusa@polito.it; phone +39 011 090 6900; fax +39 011 090 6999; www.polito.it

Relation between pull-in and pull-out voltages, respectively, with temperature conditions were often investigated. Nevertheless, it looks that trends detected by several papers are different if variation of pull-in voltage is monitored for increasing values of temperature. Some authors found increased values of pull-in voltage<sup>[7]</sup>, some others a poor dependence upon temperature, at least for at the very beginning of heating process<sup>[41]</sup>, while several authors are prone to consider a decreased pull-in voltage for higher values of temperature, or even variable trends depending on the superposition of several effects<sup>[15,17,31]</sup>. Many references include numerical and experimental results which look basically consistent, although assumptions governing proposed models and procedures very often take into account only some of the superimposed effects applied to the technical problem herein discussed, thus leading to divergent conclusions. Moreover, several phenomena give different results, when they are superimposed to microsystems where relative dimensions are different or loading sequence over time is different. Authors are therefore motivated by design of a new experimental facility aimed at investigating structural, electrical and thermal reliability of microbridges in classifying the observations already performed in the literature and relating them with geometrical parameters and mechanical properties of tested microdevices. This analysis was tentatively performed by means of some numerical and experimental results obtained on a set of microswitch prototypes. Some basic outlines are drawn and compared to those proposed in the literature.

## 2. METHODOLOGIES

A sort of phenomenological analysis of the coupled electro-thermo-mechanical behavior of RF-switch was performed. A numerical investigation was implemented. Finite Element Method was selected to analyze the multiple coupling occurring into a reference geometry of microbridge electrostatically actuated. ANSYS® code was mainly used, by resorting to plane models of clamped-clamped microbeams discretized by shell elements and coupled with electric field by means of transition elements, available into the commercial code. A simultaneous analysis of electromechanical and contact effects, respectively, when microbeam is deflected towards the fixed electrode was performed. Some geometries were investigated, although results here documented apply just for a set of microbridges, represented in Fig.1 and having geometrical properties described by Table 1. It is worthy noticing that plane models in FEM do not assure a perfect prediction of electromechanically coupled behavior of MEMS for all configurations, because of some three dimensional effects, including fringing of electric field<sup>[12,20]</sup>. Nevertheless, according to previous investigations performed by the authors, this approach is effective when ratios among RF-MEMS dimensions are those of tested microsystems<sup>[21,24,25]</sup>. Alternately other discretization approaches are available and may be effectively implemented, although in present study they were just used to verify consistency of FEM results<sup>[25]</sup>. Moreover, main problems in “out-of-plane” bending microbeams are related to discretization of narrow gap when a full integrated approach is applied. In this case transition elements allow a fairly good prediction of microstructure contact with fixed electrode.

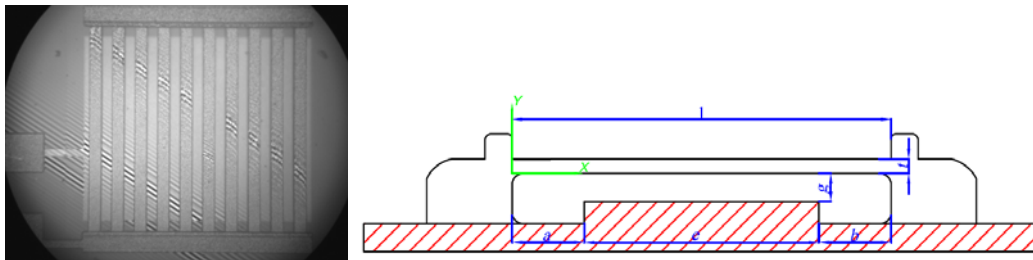


Figure 1. Picture and sketch of RF-switches set used for experimental investigations.

Table 1. Geometrical parameters and mechanical properties of tested microbridges.

Units		MEMS 1	MEMS 2	MEMS 3	MEMS 4	MEMS 5	MEMS 6	MEMS 7	MEMS 8	MEMS 9	MEMS 10
Length	[ $\mu\text{m}$ ]	544.5 $\pm$ .3	545.6 $\pm$ .3	545.6 $\pm$ .3	547.9 $\pm$ .3	546.3 $\pm$ .3	544.8 $\pm$ .3	546.9 $\pm$ .3	545.7 $\pm$ .3	547.3 $\pm$ .3	546.6 $\pm$ .3
Width	[ $\mu\text{m}$ ]	34.9 $\pm$ .3	32.5 $\pm$ .3	34.4 $\pm$ .3	35.4 $\pm$ .3	33.5 $\pm$ .3	34.5 $\pm$ .3	33.9 $\pm$ .3	32.7 $\pm$ .3	35.0 $\pm$ .3	34.8 $\pm$ .3
Thickness	[ $\mu\text{m}$ ]	2.839 $\pm$ .5 $\cdot$ 10 <sup>-4</sup>	2.932 $\pm$ .5 $\cdot$ 10 <sup>-4</sup>	2.855 $\pm$ .5 $\cdot$ 10 <sup>-4</sup>	2.936 $\pm$ .5 $\cdot$ 10 <sup>-4</sup>	2.889 $\pm$ .5 $\cdot$ 10 <sup>-4</sup>	2.901 $\pm$ .5 $\cdot$ 10 <sup>-4</sup>	2.878 $\pm$ .5 $\cdot$ 10 <sup>-4</sup>	2.920 $\pm$ .5 $\cdot$ 10 <sup>-4</sup>	2.856 $\pm$ .5 $\cdot$ 10 <sup>-4</sup>	2.854 $\pm$ .5 $\cdot$ 10 <sup>-4</sup>

For all the above described samples gap was measured and it was very close to  $3.0\pm 0.5\cdot 10^{-4}$   $\mu\text{m}$ . Microstructures were microfabricated by Foundation Bruno Kessler (FBK®) in Trento (Italy). Dimensions were measured even by means of

Zoom Surf 3D Fogale® profilometer<sup>[38,42]</sup>. Values reported in Table 1 include the equipment resolution on the wafer plane, being 0.3  $\mu\text{m}$ , while along the focal axis this value is  $0.5 \cdot 10^{-4} \mu\text{m}$ . Those resolutions are compatible with a good prediction of MEMS functionality, since gap is the most critical value for microbeam bending, since its cubic power appears within the expression of electrostatic force. Zoom Surf 3D Fogale® was used to perform a preliminary characterization of the RF-switch geometry, then to actuate the microsystem up to pull-in voltage. It analyses areas from  $100 \times 100 \mu\text{m}^2$  to  $2 \times 2 \text{mm}^2$ . Optical magnification 20x was used to achieve resolutions above mentioned. Maximum displacements up to 400  $\mu\text{m}$  can be measured, while power electronics can provide up to 200 V, up to 2MHz of frequency. To increase temperature RF-switch was mounted on a Peltier cell Fogale®, assuring a uniform heating around the MEMS, stable after few seconds, with a precision of 0.1  $^{\circ}\text{C}$  about the required temperature value, being measured by a PT100 thermal sensor, connected to a closed-loop control of cell actuation (Fig.2).



Figure 2. Experimental set-up with Peltier Cell Fogale® and Zoom Surf 3D Fogale® (courtesy of Lab. Design and characterization of microsystems– Politecnico di Torino).

Microfabrication procedure followed patented “RF Switch (RFS) Surface Micromachining” process, described in<sup>[8,23]</sup>. Material is Gold, selected to have a good electric conduction with a reduced sensitivity to wear and corrosion. Material properties certified by microfabricator are Young modulus,  $E = 98.5 \text{ GPa}$ , density,  $\rho = 19.32 \cdot 10^{-15} \text{ kg}/\mu\text{m}^3$ , Poisson coefficient,  $\nu = 0.42$  and thermal expansion coefficient,  $\alpha = 14.3 \cdot 10^{-6} \text{ }^{\circ}\text{C}^{-1}$ . Strength of material was fully characterized in<sup>[33]</sup>.

### 3. ANALYSIS OF STAND-ALONE CONFIGURATION

#### 3.1 Preliminary remarks

RF-switch layout is depicted in Fig.1. Structure is basically a very thin and deformable gold strip, clamped at both its ends by solid and massive anchors. Fixed electrode looks massive and its dimensions are defined as well as surface on which microbeam is bent by electromechanical actuation. Some aspect ratios are crucial to characterize the MEMS geometry. In particular ratios between strip length and width, length and gap, length and thickness, as well as thickness and gap are all important to define the structural behaviour of the RF-MEMS. In this case gap is small if compared to microbeam length, which is fairly large with respect to microswitch width and thickness. Three main consequences may be foreseen. Anchors should not have a compliance comparable to that of microbeam, while it happens in<sup>[18]</sup>. Cross section variation between anchor and microbeam leads to have a stress concentration around clamp, very important in fatigue tests<sup>[33]</sup>. Narrow gap allows to have in general small flexural displacements of microbeam, when axial loading does not superimpose to bending moment<sup>[12]</sup>. Nevertheless, from the computational point of view, narrow gap usually introduces some difficulties in dielectric region meshing, if Finite Element Method is applied<sup>[20,21]</sup>. Dimensions of fixed electrode provide a good contact surface, after pull-in occurring, if compared to microswitch length. Other examples in the literature show different aspect ratios, nevertheless comments above proposed may help to classify the selected layout. Large gaps may induce large displacement and consequently a fairly nonlinear structural behaviour of microbeam, but meshing dielectric region within gap looks easier, because stretching effects and elements distortion can be avoided<sup>[37]</sup>. It is worthy noticing that stress concentration around the clamp can significantly increase danger of yielding or even cracking in critical cross section, while additional tensile loading applied to microbeam may cause a

nonlinear structural behaviour, although flexural displacements remain quite small, as it was deeply investigated by authors in<sup>[20,21]</sup>.

### 3.2 Residual stress and microswitch structural stiffness

If RF-switch behaviour is analysed since its first actuation, some boundary conditions can motivate a difference between the computed pull-in voltage, at which electromechanical force overcomes elastic restoring force of the microstructure, and the actual value often found during testing<sup>[5,6,7,9,10]</sup>. Microbridge is usually referred to as statically indeterminate<sup>[11]</sup> because clamps inhibit a number of degrees of freedom larger than six, associated to rigid body seen as a free solid in space<sup>[11]</sup>. This condition motivates why after microfabrication, sometimes residual stress occurs within the microsystem structure. Microfabrication process sometimes causes difference in strain distribution between MEMS material and sacrificial layers. In case of microcantilever this effect is evident, because free end of microbeam after release is displaced from line axis, showing an initial curvature<sup>[8]</sup>. It is easily measured by profiling system and taken into account for modelling activity<sup>[42]</sup>. When both ends are clamped, microbeam rotation is inhibited and residual strain storage is converted into an initial amount of stress, stretching the MEMS structure along line axis, described by coordinate  $x$ :

$$\sigma_{xx} = E \Delta\alpha \Delta T \quad (1)$$

being  $E$  the Young modulus and  $\nu$  the Poisson coefficient of gold, respectively, while  $\Delta\alpha$  and  $\Delta T$  describe differences between thermal expansion coefficients and temperatures of gold and substrate materials, respectively<sup>[8]</sup>. Usually residual stress is tensile, therefore RF-switch geometry looks like unloaded. Unfortunately, residual tensile stress affects mechanical coupling between axial and flexural behaviours. Axial loading increases the restoring action applied by the microsystem when it undergoes bending moment, due to electromechanical actuation, leading to a reduced capability of deflection towards fixed electrode. An increased value of pull-in voltage is found. Relation among flexural displacement,  $w$ , axial displacement,  $u$ , and axial loading,  $N$ , is nonlinear:

$$N = EA \left[ \frac{\partial u}{\partial x} + \frac{1}{2} \left( \frac{\partial w}{\partial x} \right)^2 \right] \quad (2)$$

and includes axial stiffness of microbridge,  $EA$ , where  $A$  is the area of cross section. System looks like stiffened<sup>[20]</sup>. This phenomenon is very well known and usually taken into account<sup>[3,15,17,22]</sup>, with few exceptions<sup>[7]</sup>. For instance, test cases described in Table 1 did show an increased value of pull-in voltage, even at first actuation, if compared to values simply computed according to classical references<sup>[5,19]</sup>. Provided that geometrical dimensions were sufficiently precisely measured, this result could be related either to an existing axial loading, like in case of tensile residual stress, or to an imprecise measurement of elastic properties of gold, after microfabrication. Actually presence of several microcantilever samples on the same wafer where microswitches were processed, allowed verifying and measuring elastic properties and detecting their first resonance frequency and pull-in voltage, as in<sup>[22,24]</sup>. Resonance frequency and pull-in voltage are easily related to elastic properties of material. Both those inputs lead to verify the Young modulus of gold certified by the microfabricator, within a tolerance of few percents. Small differences among samples did not motivate large mismatch of values between actual pull-in voltage, about 70 V, and numerical prediction, corresponding to 35 V. Provided that Silicon and poly-Silicon materials exhibit an appreciable sensitivity of thermal expansion coefficient and Young modulus on temperature, which becomes strongly nonlinear above a temperature threshold<sup>[29]</sup>, in case of gold this dependence is far less effective according to experiments described by Collard<sup>[2]</sup>. Between 23° and 120° C, gold used for microfabrication looks exhibiting a linear variation of the Young modulus with increasing temperature. Value decreases at 120° C of 2% of the magnitude exhibited at room temperature. This change is comparable to error in direct measurement performed by means of above mentioned procedures. Residual stress could be identified on samples by means of a dynamic test, based on an experimental detection of the first resonance frequency. Those experiments demonstrated that at least a residual stress level about 25-30 MPa could motivate value of pull-in voltage detected in direct measurement. It is worthy noticing that residual stress are not stable over time, especially when structure is simultaneously excited by mechanical and thermal loading. Temperature may induce a relaxation effect on residual stress<sup>[44,45]</sup>, so as after few days or weeks their effect looks vanishing as it was demonstrated by Margesin<sup>[8]</sup>. This additional variation over time motivates significant differences in pull-in and pull-out values after a defined period<sup>[7]</sup>.

### 3.3 Heating of electromechanical uncoupled system

More complicated is case in which heating occurs even before that RF-switch is actuated. Superposition of residual stress and heating phenomenon changes quite a lot the resulting static and dynamic response of microbridge. To describe more in details this technical problem, clearly detected for instance in<sup>[43]</sup> although it was not completely modelled, a preliminary analysis of pure thermomechanical coupling was performed. If temperature increases all around the RF-MEMS, a uniform dilatation of microbeam is imposed, being inhibited by anchors. Compressive stress grows up and induces an axial load just opposite to the effect due to tensile residual stress. Theoretically as well as every numerical code suggests this compressive load does not change the microbeam shape, as well as some author refers, even recently<sup>[41]</sup>. In real systems behaviour is different. For instance, test case for a significant increasing of environmental temperature, i.e. from 25°C to 70°C, shows deformed shape depicted in Fig.3. It is upwards, with respect of fixed electrode. This result is quite common<sup>[3,6,8]</sup>, although sometimes deflection occurs towards the shortcircuit<sup>[18]</sup>.

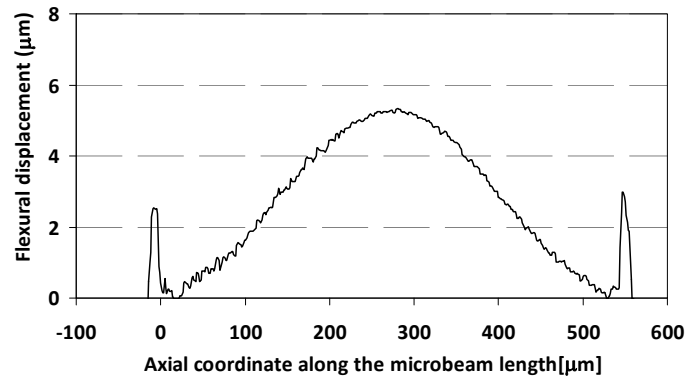


Figure 3. Microswitch profile detected by Zoom Surf 3D Fogale® on tested sample, for a temperature increasing

Above mentioned differences are compatible with some boundary conditions. Deformed shape may be motivated by non symmetric layout of anchors, imposing even a little difference in allowed rotation in deflection when flexural displacement is respectively upwards or downwards. Small imperfections in microbeam structure, i.e. small eccentricities of line axis, may lead to a preferable direction for bending. Residual stress gradient across microswitch thickness as well as a temperature difference between upper and lower surfaces of microbeam may induce a defined deformation. Moreover, microstructure slenderness may allow buckling phenomenon under compression, if axial load applied overcomes critical load for elastic instability. In that case microbeam restoring force is consistently lowered or even null, at least up to structure is unloaded. Numerical investigations performed by means of FEM (Finite Element Method) and some preliminary experiments allow describing those effects. First at all a basic distinction has to be performed between elastic deformation and partially plastic deformation, then, in case of elastic, has to be checked whether buckling could occur. If only heating operation is considered, ideally uncoupled from electromechanical actuation, some design references can be easily found out.

A numerical investigation on test case, whose results are plotted in Fig.4, demonstrates that non symmetric layout of anchors, actually plays an increasing role upon maximum flexural displacement of microbridge, as larger is curvature of detailed profile of anchor just around the clamp and shorter is microbridge. Larger values of radius  $r$  are associated with a more evident difference in flexural displacements of microbeam, when deflections occurs upwards and downwards, respectively. Nevertheless, this difference is poorly appreciable for higher values of microbeam length, for given gap and thickness. It looks insufficient to motivate a repetitive tendency of microstructure to bend along a preferable direction, except for buckling, in which even a small difference in apparent rotational stiffness at the anchor like results show in test case may induce collapse in a defined direction.

Larger effects are usually detected if residual stress is present on microbeam and if it shows a certain gradient along thickness direction<sup>[8,20,21]</sup>. This issue makes relevant evaluating residual stress distribution on the structure after microfabrication process when microtechnological characterization of MEMS is performed<sup>[8]</sup>.

Modelling this stress distribution to include its effects in dynamic analysis of electromechanically coupled MEMS is possible, but an effective prediction of stress gradients due to microfabrication process along thickness direction is practically impossible without a detailed inspection before operation<sup>[20,21]</sup>.

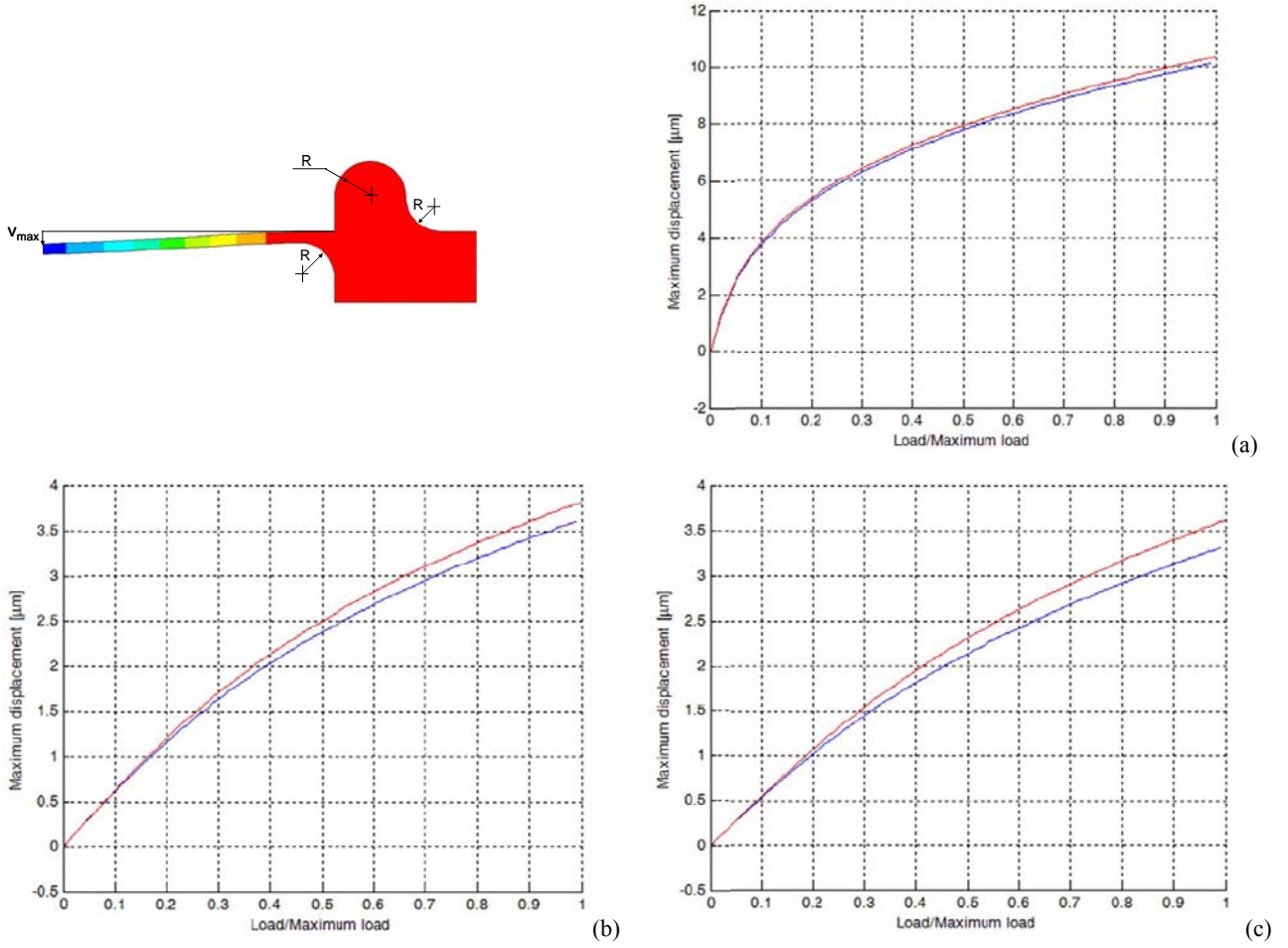


Figure 4. Flexural displacement analysis on test case and details of massive anchor maximum flexural displacement in ideally unlimited deflection of microbridge in bending is described as a function of non dimensional load applied for (a) nominal dimensions of samples and  $r = 5 \mu\text{m}$  (b) length  $200 \mu\text{m}$  and  $r = 5 \mu\text{m}$  (c) length  $200 \mu\text{m}$  and  $r = 10 \mu\text{m}$ . Upper curves describe upwards deflection while lower curves describe downwards flexural displacements.

Definitely simpler is prediction of mechanical coupling between flexural and axial loading, when temperature gradients are applied across microbeam section. Stress along line axis,  $\sigma_{xx}$ , is computed as follows

$$\sigma_{xx} = -\alpha E \frac{2\Delta T}{h} y \quad (3)$$

being  $\Delta T$  temperature difference between upper and lower surface,  $y$  direction along beam thickness,  $h$ . Higher values of temperature on lower surface induce a compressive loading, while upper surface is stretched. In test case of Fig.3 residual stress was detected, as above mentioned, but larger effects were due a superposition of two effects of temperature. Uniform heating of microbridge induced a pure compressive loading of structure, up to a critical value at which buckling occurred. Direction of flexural displacement was motivated by a minor rotational inertia of microbeam in out-of-plane bending, with respect of wafer layer, and to a slight difference of temperature between upper and lower surfaces, respectively, motivated by location of Peltier cell under the MEMS frame. Because of microstructure slenderness buckling phenomenon under compression could even occur.

### 3.4 Thermomechanical buckling and spontaneous pull-in

It is well known that elastic instability occurs in case of slender beams under compression, when compressive load overcomes beam restoring force in bending. According to classic references<sup>[1]</sup> critical load,  $P_{cr}$ , is reached when microbridge is simply heated up to a critical temperature  $T^*$ , sufficient to induce a required stress to buckling. Temperature  $T^*$  can be computed by equalling critical and thermal loads, respectively as follows:

$$P_{cr} = \frac{4\pi^2 EI}{L^2}; P_{term} = \alpha(T^* - T_0)EA; T^* = T_0 + \frac{4\pi^2 I}{\alpha A L^2} = T_0 + \frac{4\pi^2 bh^3 / 12}{\alpha L^2 bh} = T_0 + \frac{1}{3\alpha} \left( \frac{\pi h}{L} \right)^2 \quad (4)$$

where symbols meaning is microbeam length,  $L$ , second order moment of area (transversal and minimum) of cross section,  $I$ , initial or reference temperature,  $T_0$ , threshold temperature,  $T^*$ , cross section area,  $A$ , thermal expansion coefficient of gold,  $\alpha$ . Test case has rectangular cross section with dimensions  $b$  and  $h$ . Dimensions described in Table 1, allow computing preliminarily critical load,  $P_{cr} = 1020 \mu\text{N}$ , as well as threshold temperature,  $T^* = 30^\circ\text{C}$ , i.e.  $\Delta T = 7^\circ\text{C}$ . Assuming that operational range for gold RF-MEMS goes approximately up to  $70\text{-}120^\circ\text{C}$ , this threshold is included. Therefore, buckling can occur even in operating condition. Post-buckling behaviour has to be considered and predicted. An effective design approach was developed and tested in<sup>[26]</sup>. Rayleigh-Ritz method was there used to solve the proposed elastic problem. Boundary conditions were applied by imposing effects of constraints, then flexural displacement was computed at middle-span section,  $x = L/2$ , by identifying thermal loading required to induce it. Lateral microbeam displacement,  $w$ , is there assumed to be:

$$w(x) = \frac{a}{2} \left( 1 - \cos \frac{2\pi x}{L} \right) \quad (5)$$

which allows computing applied load,  $P_{TOT}$ , and axial displacement,  $u$ . In case of clamped-clamped microbeam following expressions can be derived:

$$P_{ad} = \frac{\pi^2 a^2 EI}{4L^2 r^2}; u(x) = \frac{a^2 \pi}{16L} \sin \frac{4\pi x}{L} \quad (6)$$

being coefficient  $a$  amplitude of function  $w(x)$  in Eq.(5), which describes flexural displacement of middle-span cross section, while  $r = (I/A)^{0.5}$ . For given  $P_{ad}$  threshold temperature is easily computed. Actually total load,  $P_{TOT}$ , can be interpreted as a sum of critical loading for buckling,  $P_{cr}$ , and additional contribution, for post-buckling,  $P_{ad}$ . Practically, if applied load is computed for increasing values of  $a$ , i.e. of flexural displacement, Eq.(6) allows identifying corresponding temperature,  $T$ , as follows:

$$T(a) = T_0 + \frac{1}{3\alpha} \left( \frac{\pi h}{L} \right)^2 \left( 1 + \frac{12a^2}{16h^2} \right) = T_0 + T^* + \frac{1}{3\alpha} \left( \frac{\pi h}{L} \right)^2 \left( \frac{12a^2}{16h^2} \right) = T_0 + T^* + \frac{\pi^2 a^2}{4\alpha L^2} \quad (7)$$

In Eq.(7) three components can be found. Reference temperature,  $T_0$ , corresponds to unloaded and stand-alone configuration. Temperature  $T^*$  is required to increase deflection of microbridge up to buckling threshold. Last contribution gives additional deflection caused by post-buckling loading as a function of material, geometry and load parameters. Although it may be considered trivial, this solution gives easily a prediction of microbridge deflection for given temperature. Obviously if microbeam is deflected by buckling before electromechanical actuation, its response to electric field is significantly different as well as pull-in voltage. Provided that even from that deformed shape actuation is sufficiently effective to pull-in the microbridge, two behaviours were detected in the literature. Buckling usually does not correspond directly to plastic deformation, if stress does not exceed yielding value. Actually, very often when loads are removed restoring actions bring structure to original shape, without any plastic strain. This principle is widely used in deployable structures<sup>[46]</sup>. Nevertheless, it was even observed that after post-buckling behaviour, when electromechanical actuation is applied, microbridge exhibits a very fast pull-in, associated to an almost rigid body rotation about anchors because stresses are locally sufficiently concentrated to induce initial cracks<sup>[6]</sup>. It depends on the amount of stress applied at clamps by deflection and axial to flexural coupling. Few cases of failed microbridges prone to



spontaneous pull-in after microfabrication process were found in the literature and associated to temperature increasing. Actually, in that case imperfections, thermal effects, residual stress and additional process consequences induced downwards bending of microbridge instead of upwards displacement, even for a small increment of temperature. Deflection was sufficient to bring deformed shape in contact with fixed electrode and accidentally shortcircuited. Therefore pull-in looks to be surprisingly null, because structure is actuated already in wide contact with lower electrode<sup>[7]</sup>. If microstructure is kept in a deformed configuration at a sufficiently high temperature for long time, creep phenomenon occurs and strain gradually increases, even at constant loading condition. Material thermomechanical tests are mainly aimed at characterize all those parameters for a coherent creep prediction, being significantly affected by all the superimposed effects here above described.

Trends above described in buckling can be numerically predicted in test case by assuming a very small initial elastic eccentricity of middle span cross section, either upwards and downwards respectively. As Fig.5 shows a small increment of temperature induces in first case mentioned a deformed shape upwards referred to as 'a', up to buckling monitored in Fig.3 by Zoom Surf 3D Fogale®, occurring when temperature is higher than  $T^*$ . Opposite condition corresponds to case 'b' in Fig.5. It can be remarked that spontaneous pull-in, thermally excited in absence of electromechanical actuation, brings in contact with lower electrode the microstructure. Contact modifies boundary conditions and constraints, so as additional temperature increasing causes a larger contact on the fixed electrode surface.

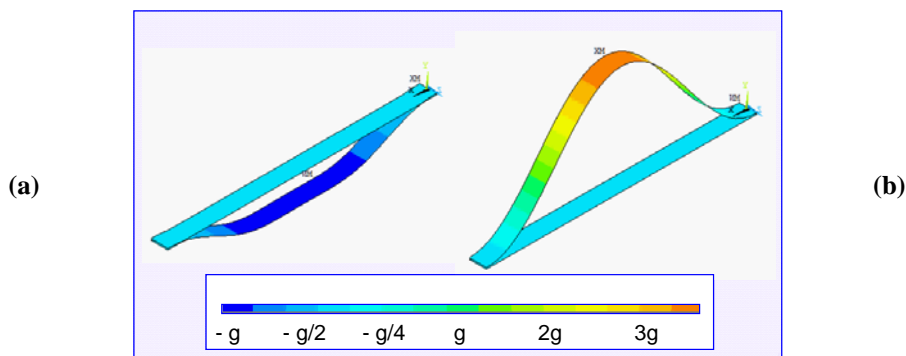


Figure 5. Numerical investigations performed on test case to predict flexural displacement in case of increasing temperature up to buckling threshold with (a) contact with lower electrode (b) free bending out-of-plane (displacement units are shown as a function of initial gap,  $g$ , and magnified).

### 3.5 Critical issues of characterization of stand-alone configuration

This preliminary overview allows drawing some relevant remarks.

1) Apparent undeformed shape of microbridge after microfabrication process does not necessarily correspond to unloaded configuration, since residual stress may occur. It is usually tensile, often relevant in amplitude, showing a gradient across the microbeam thickness, thus motivating why structure is prone to bent more upwards than downwards when temperature increases and applies compressive or slightly bending loads. If material and geometrical properties of RF-switch were previously characterized, a dynamic test may be used to identify resonance frequencies and related amount of residual tensile stress present, thanks to mechanical coupling between axial and flexural responses. Rather difficult is measuring stress gradient across microbeam thickness, without contribution of microfabricator at least when microscopy equipments are used to perform structural reliability testing.

2) Tensile residual stress induces a sort of stiffening effect on the microsystem, thus increasing the amount of voltage required to reach pull-in. Nevertheless, its effect is usually antagonist of thermal loading, which induces a compressive axial load on the microbeam structure, thus tentatively decreasing pull-in action required. Moreover, as long as heating applies to microsystem combined with mechanical loading, residual stress is relaxed up to be vanishing after a defined time. Balance between residual stress and uniform temperature distribution is prone to change significantly over time. Therefore short period, mid term and long term experimental observations performed on the same RF-switch in operation, documented in the literature, may be understandably different and even consistent.

3) Gold looks less sensitive on material elastic and thermal properties variations with temperature than silicon and related materials, if temperature range spans from room and 70-120°C. Nevertheless, it is fairly simple realizing by

means of analytical models proposed in Eqs.(4) and (7) that even in presence of pure heating without electromechanical coupling, buckling phenomenon may lead to have large deformed shapes of microbridge. In particular, for test case dimensions, this phenomenon affects behaviour within the temperature operating range. If microbeam displacement is downwards, shortcircuit is easily found and potentially RF-switch failures occurs at a very beginning of actuation. When displacement is upwards deformation may be larger, sometimes leading to have at least some microbeam cross sections under a consistent bending stress, which may reach yielding condition and cause plastic strain.

4) Open question in the literature is whether buckling phenomenon increases or decreases either pull-in or pull-out conditions. Surely null pull-in voltage looks applicable to case of downwards deflected microbeam, while only coupled electro-thermo-mechanical modelling may suggest what happens in case of upwards deflection.

5) Microbeam structure never exhibits a preference in flexural behaviour to bend upwards or downwards if an ideal model is considered, while temperature gradients along thickness as well as imperfections, eccentricities and residual stress distribution or material homogeneities defects motivate such as real behaviour in practice. Anchors layout is important but somehow not dominant in defining this aspect. When anchor structural stiffness is comparable with microbeam stiffness, the whole structure has to be modelled. This condition occurs in case of highly compliant anchors<sup>[18]</sup> or even of test sample, where massive anchors are applied but a suitable ratio between radii of shape curvatures and beam length may lead to a local stiffness comparable in deformable structure and constraint, respectively.

6) Superposition of several effects such those above mentioned give different results depending on microsystem aspect ratios and dimensions, since each phenomenon may be potentially dominant among the others.

## 4. RF-SWITCH OPERATION WITH ELECTRO-THERMO-MECHANICAL COUPLING

### 4.1 Buckling and pull-in and pull-out phenomena

To investigate RF-switch at least at its first actuation, a complete nonlinear electro-thermo-mechanical model of test cases described in Table 1 was developed in ANSYS®. Some typical sequential actuations over time were simulated. Results are shown for average values of test case and design parameters were assumed to be  $L = 540 \mu\text{m}$ ,  $b = 34 \mu\text{m}$ ,  $h = 3 \mu\text{m}$ ,  $E = 98500 \text{ MPa}$ ,  $\nu = 0.42$ ,  $\alpha = 14.3 \cdot 10^{-6} \text{ K}^{-1}$  and gap  $g = 2.9 \mu\text{m}$ . To investigate superposition of effects previously described a sequence of thermal and electromechanical loading conditions was applied. Because of strong axial to flexural coupling iterative solution for coupled behaviors was implemented according to procedures developed by authors in<sup>[20,21,24,25,38,42]</sup>. Among several investigations the most impressive results will be herein described.

#### Thermal post-buckling and pull-in

If heating is used to induce pull-in effect on test case, deformed shape completely in contact with fixed electrode surface is found when applied voltage is 34 V. When environmental temperature is increased before actuation up to 40°C, thus overcoming  $T^*$  for buckling and deformation is upwards (Fig.5.b), pull-in voltage increases just up to 40 V. This results sounds as a compromise between two effects. In post buckling deformed shape is under the effect of compressive load, so as axial contribution in axial to flexural coupling tends to soften microbeam, but gap distribution with respect to fixed electrode is significantly increased and electromechanical force is considerably less effective. If microbeam is deflected downwards, pull-in voltage looks null, but electromechanical actuation may increase contact surface on fixed electrode.

#### Thermal secondary buckling and spontaneous pull-out

In Fig.6 a loading sequence to perform a flexural displacement analysis is proposed. Sample was initially heated up to  $\Delta T = 10^\circ\text{C}$  and boundary conditions were applied to induce a positive deflection towards fixed electrode, in case of complete buckling. Microbeam bends down, but it does not touch fixed electrode. It is then sufficient applying an actuation voltage of 15 V to reach a contact between microbridge and electrode. All phenomena associated with contact are activated<sup>[15]</sup>. In particular, from the electrical point of view all typical forces, associated to charges attraction and low range interaction are assumed to be effective<sup>[37]</sup>. Moreover, when several loading cycles are performed even charge entrapment occurs, which often requires a pull-out voltage to help restoring force to bring microbridge in undeformed configuration. In this case it was assumed that in presence of constant voltage temperature increases because of shortcircuit. Joule effect applies at least to surface of microswitch in contact with lower electrode. It can be remarked that in real actuation frequency is fairly high, actuation is dynamic and contact is closed for short periods of time, but so often that usually an average heating effect is measured like if microsystem were almost continuously heated<sup>[3]</sup>. Model assumes that temperature gradually increases, up to a condition for which shape of microbeam is modified as Fig.6

shows in first column down left. As in higher frequency vibration modes several nodes appear in deformed shape. So far they exert an action on contact surface. Suddenly microstructure snaps up so fast that a larger flexural displacement is achieved (Fig.6, column right). In principle displacement can reach significant amplitude, in practice this effect is limited by strength of material.

As this investigation shows spontaneous pull-out may even occur, thus motivating some observations proposed in the literature<sup>[15]</sup>. Temperature increment  $\Delta T = 90^\circ\text{C}$  required in test case to reach this secondary buckling, was fairly high, but approximately still included into operational range. It can be remarked that this simulation did not include residual stress, nor additional forces associated with short-circuited configuration, which may increase this value. Pull-out voltage can evenly excite buckling upwards as it was found out at the end of sequence.

### Stress in electro-thermo-mechanical coupling

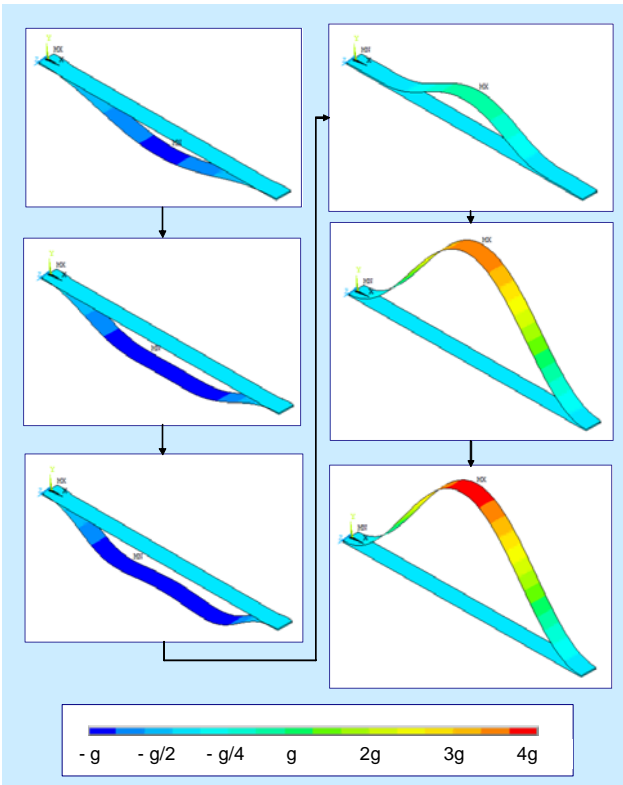


Figure 6: FEM simulation of primary and secondary buckling of microbridge with electro-thermo-mechanical coupling.

As it was previously remarked some effects on pull-in and pull-out conditions are strictly related to stress concentration and eventually to yielding phenomenon. To investigate this issue a preliminary stress computation was performed for the simulated sequence of loading previously analyzed. Following Fig.7 shows some relevant results, concerning at least bending normal stress applied along line axis direction, namely  $x$  in these computations.

All maps show a stress concentration on both the upper and lower surfaces, respectively, just in correspondence of clamps on both sides shown in each row of Fig.7. As usual in bending one surface is mainly under tensile effect, while the opposite is compressed. At first buckling, maximum tensile stress reaches 17 MPa on the upper surface, while compression is even large on lower face, up to 36 MPa. At pull-in flexural displacements are larger so as upper tensile stress achieves 70 MPa and lower compression is about 80 MPa. Contact mechanics significantly increases stress levels at interface with fixed electrode. In particular, close to fixed electrode edges, on upper surface a large compression is appreciated and values are about 130 MPa, while on lower surface concentration is close to clamps. For gold this value overcomes strength of material<sup>[33]</sup>, being at least twice fatigue limit<sup>[33]</sup>. It can be remarked that fixed electrode plays the role of additional support, thus unloading some parts of microbeam, where stress is considerably lowered. After second buckling stress level increases. Upper surface suffers a strong compression at clamps, while lower surface shows the same concentration but due to tensile stress. According to stress analysis and to Fig.8 where stress variations are depicted for given cross section as a function of time, it can be remarked that:

- 1) stress distribution changes significantly during RF-switch excitation, in particular order of magnitude may reach values comparable to yielding or even ultimate strength of material, if aspect ratios, material properties and dimensions are those of industrial components;
- 2) stress distribution is significantly affected by edge effects, showing irregularities due to three dimensional nature of stress state, particularly around clamps, being typically cross sections relevant for design;
- 3) contact is important for additional stress applied, in global stress distribution, in terms of supporting the deflected microbridge and helping secondary buckling snap motion.

All those configurations obviously are just a possible assumption of loading sequence for RF-switch operation. Nevertheless, even in case of different sequence over time, they can represent some critical shapes to be considered in

design and explain some interesting results proposed in the literature. Actually, previous example did not carry out a complete loading condition including residual stress, being there neglected. To analyse what happens in case of superimposed heating, buckling, residual stress and electromechanical coupling some experiments were directly performed on samples.

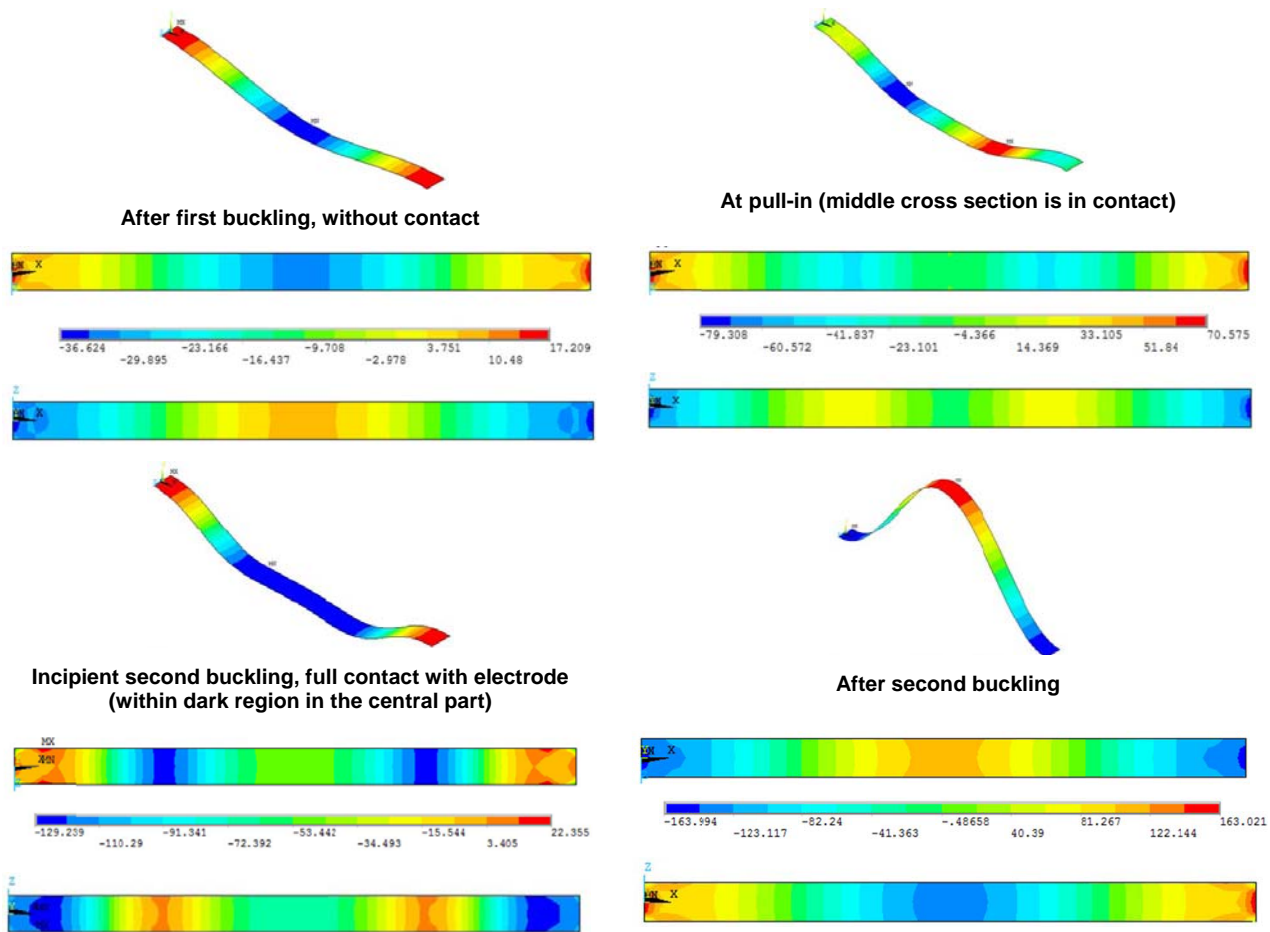


Figure 7: FEM simulation stress distribution in four relevant configurations of RF-switch. For each deformed shape, flexural displacement is shown in the upper plot, then top view of upper and lower surfaces of microbeam are shown just above and below colors legend of stress, reported in MPa units.

#### 4.2 Preliminary experiments

Tests were performed on prototypes by means of Zoom Surf 3D Fogale ® and Peltier Cell Fogale ®. All samples described by Table 1 were tested. Every microsystem was observed several times during repeated loading cycles. In this preliminary activity two sessions were planned. In a first step only thermomechanical coupling was observed and buckling. Second session was used to study pull-in phenomenon in presence of different temperature. It can be remarked that loads were applied slowly and dynamic behavior of RF-switch was not yet observed, at frequencies typical for usual operation. Nevertheless, this research step was useful to distinguish role of different phenomena, although further investigations have to be performed to predict actual behavior at high frequency.

#### Thermomechanical loops

A first screening was performed by applying increasing thermal loading due to gradual heating of RF-switch, from room temperature towards test temperature, followed by slow cooling. Since for this particular MEMS operating temperature

should not exceed 80°C a preliminary set of experiments was limited to this temperature value, although investigation could be even extended. It can be remarked that for all samples, as is for n.1 whose results are shown in Fig.9 on the left, no hysteresis occurs when heating-cooling path is followed during testing. This result demonstrates that strain is elastic, no effective damage occurs, and operation looks reversible, at least for given loading cycle, at the beginning of component operative life.

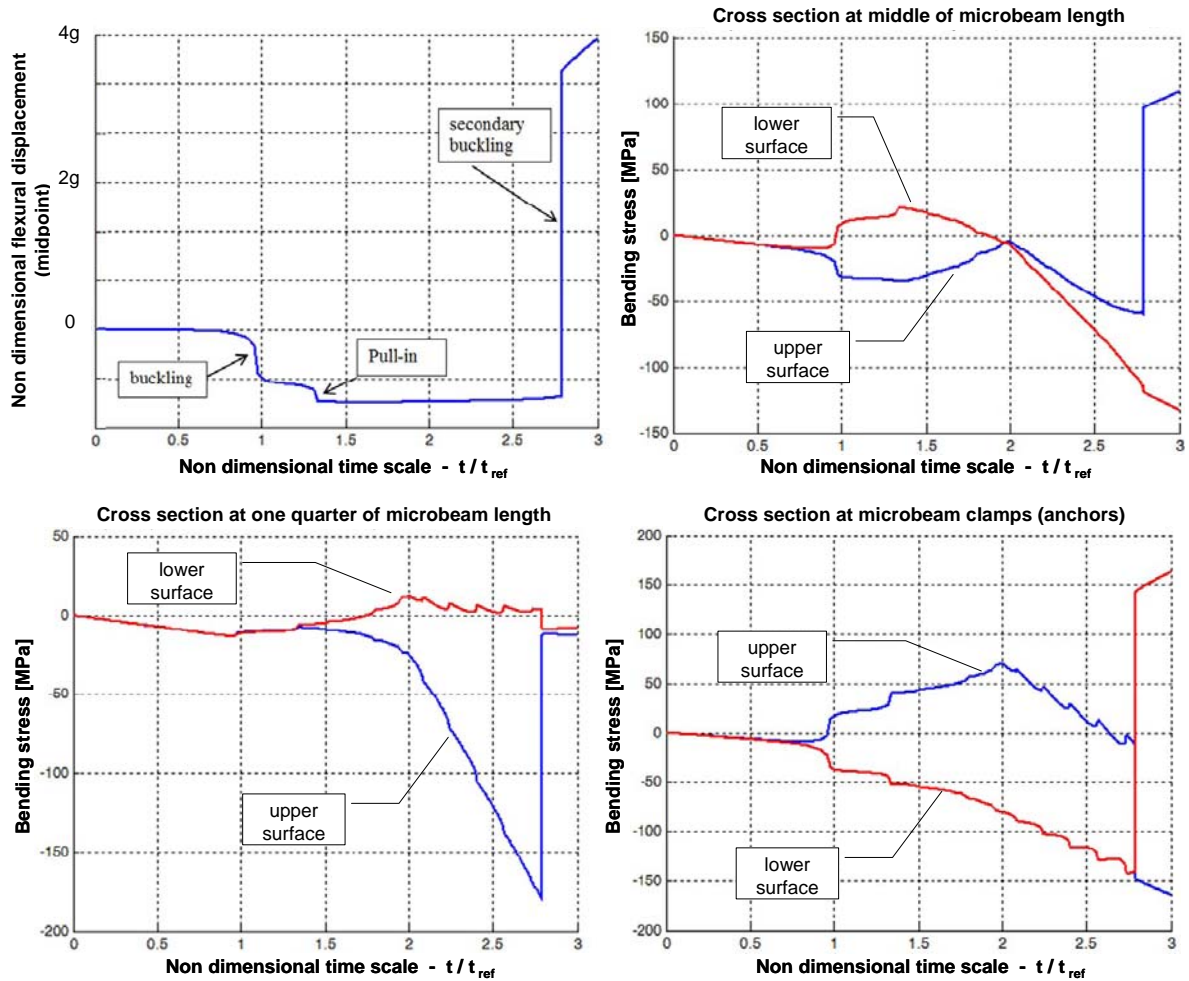


Figure 8: FEM results of stress analysis performed on test case, plotted as a function of non dimensional simulation time

### Thermomechanical buckling

Behavior of RF-switch in case of buckling and post-buckling conditions, respectively, could be directly checked for all samples, by comparing above mentioned thermomechanical loops and numerical prediction, computed by means of models proposed in Eq.(4) and Eq.(7). As Fig.9 shows on the right during microbeam heating flexural displacement increases. A first step includes small increments, mainly due to charge entrapment and electric interaction with fixed electrode, but significant displacements appear when instability threshold is overcome and buckling occurs. This transition is very easily seen in Fig.8 and 9. Above buckling threshold agreement between numerical model and experiments is good. Small dimensional differences in samples, described by Table 1, actually do not change significantly mechanical response to heating up to buckling, while above that some differences are appreciated. Nevertheless, model, implemented for average values of samples parameters is suitable to predict, at least approximately the actual behaviour of RF-switch set as it is evident in Fig.9 on right side. Moreover, threshold temperature for buckling is higher than value previously computed. This effect is due to residual tensile stress detected into samples, by dynamic

tests. Actually if expression of Eq.(7) is updated by introducing elastic stress due to residual action, approximately considered uniform across microbridge thickness, value of  $T^*$  found is about  $53^{\circ}\text{C}$  and fits experimental evidence. It can be remarked that an inverse procedure could be even based on threshold temperature detection to find out initial residual stress stored by RF-switch.

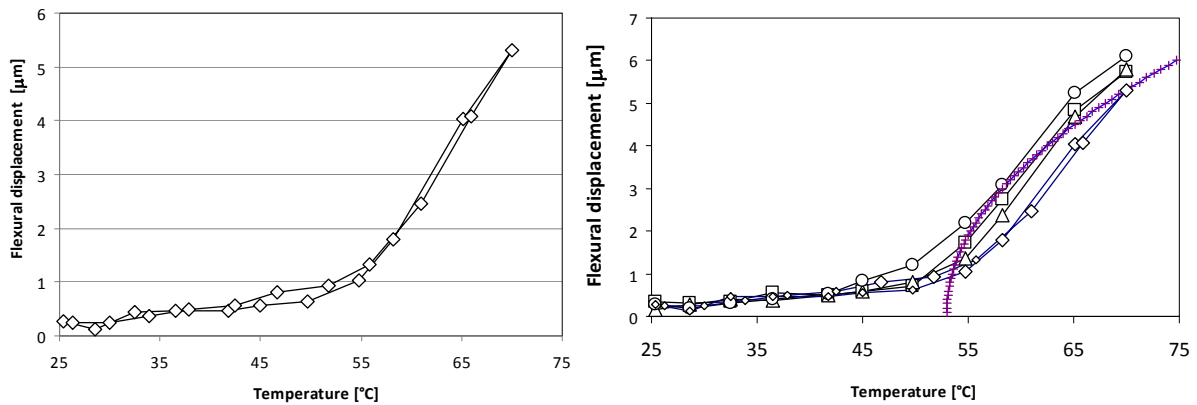


Figure 9: Flexural displacement measured by Zoom Surf 3D Fogale ® in a complete heating-cooling and post-buckling.

### Electro-thermo-mechanical loading

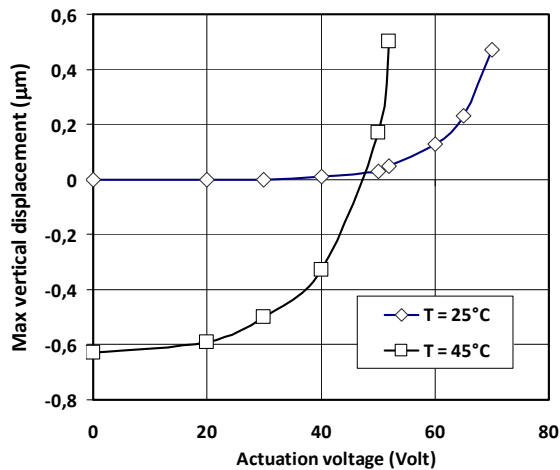


Figure 10: Experimental results of pull-in tests performed in presence of residual stress, at two different values of temperature.

To complete this preliminary analysis an integrated loading condition, including residual stress, heating and electromechanical actuation was evenly tested. Results are depicted in Fig.10. At room temperature sample shows higher value of pull-in voltage than one computed without residual stress. This is due to tensile action, stiffening axial to flexural coupling. At higher temperature, pull-in voltage decreases, at least for temperature values below buckling condition, according to Fig.9. This result is motivated by compression caused by temperature, which reduces apparent stiffness of microbeam. Nevertheless, since test temperature is still lower than buckling threshold, restoring force is decreased while gap is still sufficiently small to make electromechanical force very effective. Pull-in is consequently easily obtained. This experiment fits experience documented by several authors<sup>[10,15,31]</sup>. Nevertheless, when temperature overcomes threshold required for buckling, deformed shape becomes similar to last case depicted in Fig.6. In this condition pull-in voltage seems to be larger. Computation already stated that a certain increasing is appreciated and pull-in condition is achieved,

while in practice, on tested sample this result was hard to be reached, because of large gap exhibited by microbeam. Superposition of several effects, fringing of electric field and interaction with air, made in practice ineffective electromechanical actuation for larger values of gap. This evidence motivated some statements, apparently opposite to previously cited, which are prone to consider pull-in voltage larger in case of electro-thermo-mechanical coupling<sup>[7]</sup>. It is remarkable that in real operation dynamics superimposes to all the above mentioned phenomena and long term operation may lead to have a thermal relaxation of residual stress. Those additional contributions may change RF-switch behaviour over time. Nevertheless, preliminary experiments could clarify contests and consistency of different statements proposed in the specialized literature and could be used to design new experimental set-up for electro-thermo-mechanical reliability tests.

## 5. CONCLUSIONS

RF-switch operation is strongly affected by geometry, residual stress, temperature, buckling phenomenon and multiple coupling caused by interaction between axial and flexural behaviours and superposition of electrical, thermal and mechanical actions. A comprehensive analysis was here performed. Numerical and experimental evidences demonstrated that pull-in and pull-out voltages may be significantly changed by all those actions. Compliance and influence of massive anchors have to be evaluated case by case. Tensile residual stress may increase pull-in voltage, at least up to relaxation induced by higher temperature. Elastic and thermal properties change with temperature, more evidently in silicon than in gold material. If buckling occurs before actuation, RF-switch can be either shortcircuited or taken away from fixed electrode. Temperature induces a compressive action that decreases microbeam restoring force in pull-in, but can induce spontaneous pull-out, if secondary critical load is overcome. In practice, buckled microstructures may show larger values of pull-in voltage or yielding of material, because of large gap induced. All those observations will be carefully considered by authors in designing a new experimental set-up aimed at studying electro-thermo-mechanical reliability.

## 6. ACKNOWLEDGEMENT

Authors appreciate fundamental contributions of Prof. Aurelio Somà and Dr. Giorgio De Pasquale in experimental activities performed at Laboratory of Design and Characterization of Microsystems, at Politecnico di Torino, Italy.

## REFERENCES

- [1] Timoshenko, S. and Gere, J., [Theory of elastic stability], McGraw Hill, Tokyo, 1961.
- [2] Collard, S.M. [High temperature elastic constants of Gold single-crystals], Ph.D. thesis, Rice University, n.9136015, Houston, Texas, 1991.
- [3] Lin, L. et al., "Self-buckling of micromachined beams under resistive heating", *J.MEMS*, 9(1), (2000).
- [4] Hasiang Pan, C. "A simple method for determining linear thermal expansion coefficients of thin films", *J.Micromech. Microeng.*, 12, 548–555, (2002).
- [5] Rebeiz, G., [RF MEMS: Theory, Design, and Technology], Wiley Interscience, 2002.
- [6] Jensen, B.D., et al. "Fully integrated electrothermal multidomain modeling of RF MEMS switches", *IEEE Microwave and wireless components letters*, 13(9), (2003).
- [7] Jing, Q., [Modeling and Simulation for Design of Suspended MEMS], Ph.D. thesis, Carnegie Mellon University, Pittsburgh, Pennsylvania, 2003.
- [8] Margesin, B., et al., "Stress characterization of electroplated gold layers for low temperature surface micromachining", *Proc. IEEE/DTIP 2003*, May 2003, Mandelieu-La Napoule, France.
- [9] Reid, J. R., et al., "RF Actuation of Capacitive MEMS Switches", *IEEE MTT-S Digest*, paper TH2D-2 (2003).
- [10] Rocha, L. A., et al., "Stability of a Micromechanical Pull-In Voltage Reference", *IEEE Trans.Inst.Meas.*, 52, (2003)
- [11] Brusa, E., et al. "Modeling and prediction of the dynamic behaviour of microbeams under electrostatic load", *Anal.Int.Circ.Sign.Proc.*, 40(2), 155–164, (2004).
- [12] Collenz, A., et al., "Large deflections of microbeams under electrostatic loads", *J. Micromech. Microeng.*, 14, 365-373, (2004).
- [13] Nieminen, H., et al., "Design of a Temperature-Stable RF MEM Capacitor", *J MEMS*, 13(5), (2004)
- [14] Yan, D., et al., "Design and modeling of a MEMS bidirectional vertical thermal actuator", *J. Micromech. Microeng.*, 14, 841–850, (2004).
- [15] Zhu, Y., et al., "Effect of temperature on capacitive RF MEMS switch performance a coupled-field analysis", *J.Micromech. Microeng.*, 14, 1270–1279, (2004)
- [16] Baek, C., "Measurement of the mechanical properties of electroplated gold thin films using micromachined beam structures", *Sensors and Actuators A*, 117, 17–27, (2005).
- [17] Goldsmith, C.L., et al., "Temperature Variation of Actuation Voltage in Capacitive MEMS Switches", *IEEE Microwave Wireless Components Letters*, 15(10), (2005)
- [18] Kang, T., et al., "Low-thermal-budget and selective relaxation of stress gradients in gold micro-cantilever beams using ion implantation", *J. Micromech. Microeng.* 15, 2469–2478, (2005)
- [19] Brusa, E., "Dynamics of mechatronic systems at microscale", in [Microsystem Mechanical Design], CISM Lectures Series, Springer Verlag, 57–80, (2006).

- [20] Brusa, E., Munteanu, M., "Coupled-field FEM nonlinear dynamics analysis of continuous microsystems by non incremental approach", *Anal.Int.Circ.Sign.Proc.*, 48, 7–14, (2006).
- [21] Brusa, E., Munteanu, M., "Validation of compact models of microcantilever actuators for RF-MEMS application", *Anal.Int.Circ.Sign.Proc.*, 59, 191–199, (2006).
- [22] Espinosa, H.D., et al., "MEMS-based Material Testing Systems", in [Encyclopedia of Materials: Science and Technology], Elsevier Ltd., New York, (2006).
- [23] Subhadeep, K., et al., "Stress and resistivity analysis of electrodeposited gold films for MEMS application", *J. Microelectronics*, 37(11), 1329–1334, (2006).
- [24] Ballestra, A., et al., "Experimental characterization of electrostatically actuated inplane bending of microcantilevers", *Microsys.Tech.*, 14(7), 909–918, (2008).
- [25] Bettini, P., et al., "Static behaviour prediction of microelectrostatic actuators by discrete geometric approaches", *IEEE Trans.Magnetics*, 44(6), 1606–1609, (2008).
- [26] Gupta, R.K., et al., "Thermal post-buckling analysis of slender columns using the concept of coupled displacement field", *Int.J.Mech.Sciences*, 52, 590–594, (2008)
- [27] Tabata, O., et al., [Reliability of MEMS: Testing of Materials and Devices], Wiley-VCH, (2008).
- [28] Rezvaniyan, O., et al., "The role of creep in the time-dependent resistance of Ohmic gold contacts in radio frequency microelectromechanical system devices", *J. Applied Physics*, 104(2), (2008).
- [29] Shamsheersaz, M., et al., "Polysilicon microbeams buckling with temperature-dependent properties", *Microsys.Tech.*, 14, 957–961, (2008).
- [30] Bogner, G., et al., "Contactless thermal characterization of high temperature test chamber", *Microsys.Tech.*, 15, 1279–1285, (2009).
- [31] Palego, C., et al., "Robustness of RF MEMS Capacitive Switches With Molybdenum Membranes", *IEEE Trans. Microwave Th.Tec.*, 57(12), (2009)
- [32] Sadek, K., et al., "A Coupled Field Multiphysics Modeling Approach to Investigate RF MEMS Switch Failure Modes under Various Operational Conditions", *Sensors*, 9, 7988-8006, (2009)
- [33] Somà, A., et al., "MEMS Mechanical Fatigue: Experimental Results on Gold Microbeams", *J. MEMS Trans. ASME/IEEE*, 18, 828–835, (2009).
- [34] Szabo, P., et al., "Thermal transient characterisation of the etching quality of micro electro mechanical systems", *Microelectronics Journal*, 40, 1042–1047, (2009).
- [35] Veijola, T., et al., "Experimental validation of compact damping models of perforated MEMS devices", *Microsys.Tech.*, 15 (2), 1121–1128, (2009)
- [36] Yan, X., et al., "Anelastic Stress Relaxation in Gold Films and Its Impact on Restoring Forces in MEMS Devices", *J.MEMS*, 18(3), (2009)
- [37] Brusa, E., "Design for reliability of micromechatronic structural system" in [Micro Electro Mechanical Systems, MEMS: Technology, Fabrication Processes and Applications], Nova Science Pub. Inc., (2010).
- [38] Brusa, E., et al. "Characterization of thermo-mechanical coupling in gold microbridges", *Proc. IEEE DTIP 2010*, 5-7 May, 2010, Sevilla, Spain, 344–349.
- [39] Mahameed, R., et al. "A High-Power Temperature-Stable Electrostatic RF MEMS Capacitive Switch Based on a Thermal Buckle-Beam Design", *J.MEMS*, 19(4), (2010)
- [40] Mulloni, V., et al. "Controlling stress and stress gradient during the release process in gold suspended microstructures", *Sensors and Actuators A*, 162, 93–99, (2010)
- [41] Saeedivahdat, A., et al., "Effect of thermal stresses on stability and frequency response of a capacitive microphone", *Microelectronics Journal*, 41, 865–873, (2010).
- [42] Somà, A., et al., "Effect of residual stress on the mechanical behaviour of microswitches at pull-in threshold", *Strain*, 46 (4), 358–373, (2010)
- [43] Zamanian, M., et al., "Analysis of thermoelastic damping in microresonators by considering the stretching effect", *Int. J. Mechanical Sciences*, 52, 1366–1375, (2010)
- [44] Epp, J., et al., "Residual stress relaxation during heating of bearing rings produced in two different manufacturing chains", *J. Mat. Proc. Technology*, 211, 637–643, (2011)
- [45] Medvedeva, A., et al., "Thermally activated relaxation behaviour of shot-peened tool steels for cutting tool body applications", *Materials Science and Engineering A*, 528, 1773–1779, (2011)
- [46] Motro, R., [Anthology of structural morphology], World Scientific, Singapore, (2010).